Local orientational order in binary liquid Li-In alloys

1995 J. Phys.: Condens. Matter 7 517

(http://iopscience.iop.org/0953-8984/7/3/007)

J. Phys.: Condens. Matter 7 (1995) 517–530. Printed in the UK

Local orientational order in binary liquid Li–In alloys

Chen Kuiying, Liu Hongbo and Hu Zhuangqi

State Key Laboratory of Rapidly Solidified Alloys, Institute of Metals Research, Academia Sinica, Shenyang 110015, People's Republic of China

Received 16 May 1994, in final form 16 September 1994

Abstract. The local orientational order in binary liquid Li–In alloys at a constant temperature has been systematically studied using molecular dynamics simulations combined with potential mapping techniques. The generalized non-local model pseudopotential theory has been chosen as the fundamental theory for our calculation. Both the orientational order parameters and pair analysis approach have been adopted to examine the characterization of structures in binary liquid Li–In alloys. It demonstrates that the mapping procedure produces a significant image enhancement of the short-range order, and the third-order invariant of the spherical harmonics is much more sensitive to the icosahedral symmetry than is the quadratic invariant. In addition, the bonded pairs with various symmetries, icosahedra, defective icosahedra, etc, formed in liquid Li–In alloys are also examined and the relationship between these quantities and compositions are investigated. The results further show that distributions of the attractive part of the potentials play an important role in characterizing liquid structures. Finally, a detailed discussion of the results has been given.

1. Introduction

The microstructure and dynamics behaviour of liquid metals are still current active topics of research in the field of condensed-matter physics. For several decades, numerous attempts have been made to reveal the relationship between the structure and force in the liquid phase. It is difficult to make an extensive study of this problem because the local order in the liquid under normal conditions of thermal equilibrium reflects a compromise between the energetically most favourable packing and thermally induced distortions [1], and conventional energy minimization routines are often inappropriate [2].

In 1984, Stillinger and Weber [3–5], proposed a new approach which may allow us to establish a unique structure–force relationship. The basic idea is to separate energy and geometric packing considerations from the thermal excitations. This is achieved by mapping the instantaneous configurations of the liquid onto nearby potential energy minima. The appropriate mapping is achieved by the steepest-descent algorithm via a steepest-gradient path to a nearby configuration at which the potential energy is locally a minimum, and the inherent structure was verified for various systems considered by Stillinger and Weber [6].

It is well known that the radial pair distribution functions (RDFs) convey basic geometric information about the atom arrangement in materials and thus have been widely used in the research for disordered systems, such as in liquids, supercooled liquids and in amorphous solids. However, for the physical origin of the second-peak splitting of the RDF in metallic glasses and of the anomalous structure such as a shoulder appearing on the principal peak of the structure factor, no apparent picture can be derived from the RDF at the atomic level. The remarks made by Broughton *et al* [7] on the RDF may be more relevant. Broughton *et al* [7] argued that, since the conventional RDF is determined on the basis

0953-8984/95/030517+14$19.50

of the hypothesis that all pairs are assumed with equal weight in the average without regard to their orientation, much information is lost in the RDF. Thus the structure of a liquid cannot be completely described by only the RDF. In contrast with this, several studies have been made by Steinhardt *et al* [8, 9] on the basis of the bond orientational order approach which has now been widely applied in the relevant area, e.g. to supercooled liquids and amorphous solids. The method can indeed provide a useful insight into our understanding of the microstructure of liquids at the atomic level. Another interesting method called the pair analysis (PA) technique developed by Honeycutt and Andersen [10] is thought to be capable of providing an apparently physical picture about the atom arrangement. On the basis of this method, Lu and Szpunar [11] and Wang and co-workers [12–14] have examined the characteristics of the liquid-to-glass transition and give the trends of various symmetries of bonded pairs defined by the PA approach. Qi and Wang [15] first employed the PA technique to detect and count icosahedra, defective icosahedra and Frank–Kasper (FK) polyhedra in supercooled liquid and amorphous $Mg_{30}Ca_{70}$ alloy. Recently, Liu *et al* [16] have reported that the second-peak splitting of the pair correlation function in supercooled liquids and amorphous solids is due to the occurrence of the icosahedral cluster; then they further demonstrated that a shoulder appearing on the high-wavelength number side of the structure factor of pure liquid indium is associated with 1311 bonded pairs [17].

It is known that lithium is a typical simple metal and can be well described by the hard-sphere model, whereas indium is a polyvalent metal and exhibits an anomalous structure feature compared with the simple metal. Thus some interesting structures may appear when they are mixed together. Exploring these structure characteristics is the main subject of our research. In the present paper we adopted both the bond orientational order and the PA technique to reveal these features by molecular dynamics (MD) simulation combined with potential energy mapping.

2. Effective interatomic potential

In this paper we use the effective interatomic potentials derived from the generalized non-local model pseudopotential (GNMP). The derived pseudopotential contains a detailed concentration dependence. This method has been well documented elsewhere [18, 19]. The GNMP has been well applied to the investigation of liquid metallic structures, electronic transport and even liquid-to-glass transition. This is the main reason that we chose the GNMP as a fundamental of simulation. The effective pair potential derived from the GNMP takes the form

$$V_{ij}(r) = \frac{Z_{\mathrm{eff},i}Z_{\mathrm{eff},j}}{r}\left(1 - \pi^{-1}\int_0^\infty \mathrm{d}q\,[F_{ij}(q) + F_j(q)]\frac{\sin(qr)}{q}\right) \tag{1}$$

where $Z_{\mathrm{eff},i}$ and $Z_{\mathrm{eff},j}$ are the valence of effective ions; $F_{ij}(q)$ or $F_{ji}(q)$ stands for the normalized energy wavenumber characteristics. As an example, effective interatomic potentials for binary Li–In alloys at specially selected compositions are shown in figure 1. The concentration dependence of the pair potentials is very much as expected. It is clear that $V_{\mathrm{In-In}}(r)$ has a much narrower and deeper minimum than do the other two pairs and, with the increasing In concentrations, this attractive part becomes broader and shallower. At an In content of more than 70 at.%, the attractive part of potentials for unlike pairs, say Li–In pairs, however, exceeds those of the other two pairs. This large potential difference must induce structures to change on a large scale, which is the main subject that we explore. In the simulation of our research, when atomic volumes are not available in the experiment,

we determine them in the manner given by Wang and Lai [20]. The atomic volumes thus obtained for the Li–In alloys of interest are in error by an amount which is expected to be about 10% or less, as stated by Wang and Lai [20]. Hence, the interatomic potentials show a pronounced dependence upon the composition and the atomic volume of the alloys, and also the relative depths of the three potentials vary with composition.

3. Molecular dynamics simulation and potential mapping

MD simulation, first developed by Alder and Wainwright [21] and later extended by Verlet [22], is potentially capable of providing very detailed microscopic features of metals and has been used to investigate liquid structure, glass formation and several relevant aspects. In the present paper we performed a NVT MD simulation at a constant temperature (924 K) for a total of 500 particles (including different types of atoms) in a cubic box subject widely used period boundary conditions for all cell faces. The initial positions of atoms are randomly chosen, and the equations of motion of atoms are solved using the Verlet algorithm with momentum scaling. The time increment is 0.32×10^{-13} s. Typical runs take 3×10^5 steps for equilibrium in order to guarantee the equilibrium state. 20 configurations of atoms are recorded during simulation. Then the steepest-descent energy minimization procedure with the conjugate gradient is imposed on each of those configurations. Finally the PA techniques are performed in a separate program. It should be pointed out that our results are averaged over 20 configurations and the calculation is in atomic units. All the calculations were performed on a DEC 5000/125 workstation in our laboratory.

4. Geometric description of orientational order

The importance of local orientational symmetries in three dimensions was emphasized over 40 years ago by Frank [23]. Three-dimensional bond orientational order has been studied theoretically by Nelson and Toner [24]. Since then Steinhardt *et al* [9] have applied it in the simulation of a supercooled Lennard-Jones liquid and in the examination of the possibility of local and extended icosahedral bond order. For realistic metals or alloys, much less is known about their three-dimensional order. Thus, in our present research, we shall measure local orientational symmetries in the computer-generated models of binary liquid Li–In alloys. However, our attention is restricted to various icosahedral symmetries, FK polyhedra and Bernal hole polyhedra defined by the bond orientational order and the PA approach respectively.

In liquid metals, any two atoms form a bond if they are within a distance chosen to equal the first minimal positions of $g(r)$. The bond is described in terms of orientational order parameters Q_{lm}:

$$Q_{lm}(r) = Y_{lm}(\theta(r), \varphi(r)) \qquad m = -l, \ldots, 0, \ldots, l \tag{2}$$

where $Y_{lm}(\theta(r), \varphi(r))$ are spherical harmonics; θ and φ are the polar angles of the bond measured with respect to some coordinate system.

In the case of a cluster of particular interest, the averaged orientational order parameter should be considered

$$\bar{Q}_{lm}(r) = \langle Q_{lm}(r) \rangle \tag{3}$$

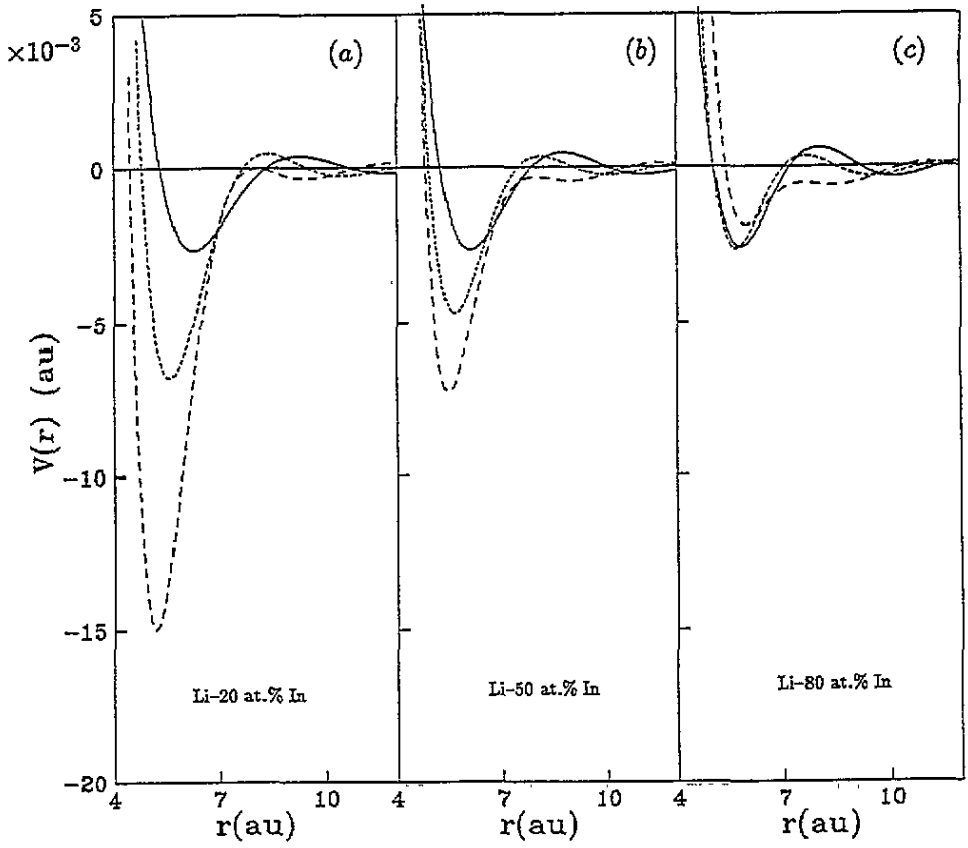

Figure 1. Effective interatomic potentials for binary liquid Li–In alloys at selected compositions and at 924 K: ——, $V_{Li-Li}(r)$; ----, $V_{Li-In}(r)$; – – –, $V_{In-In}(r)$.

where the average is taken over all bonds within the cluster. In order to eliminate the dependence of Q_{lm} on a special coordinate system, it is important to consider the rotational invariant combination

$$Q_l = \left(\frac{4\pi}{2l+1} \sum_{m=-l}^{l} |\bar{Q}_{lm}|^2 \right)^{1/2}. \tag{4}$$

It is clear to see that Q_l is a quadratic invariant of Q_{lm}. For icosahedral symmetry, it suffices to calculate the orientational order parameter $\hat{W}_6$, which is very sensitive to the icosahedral symmetry suggested by Steinhardt. $\hat{W}_6$, which is the third-order invariant of Q_{lm}, is defined as

$$\hat{W}_6 = W_6 \Big/ \left(\sum_{m=-6}^{6} |\bar{Q}_{6m}|^2 \right)^{3/2} \tag{5}$$

in which

$$W_6 = \sum_{\substack{m_1,m_2,m_3 \\ m_1+m_2+m_3=0}} \begin{bmatrix} 6 & 6 & 6 \\ m_1 & m_2 & m_3 \end{bmatrix} Q_{6m_1} Q_{6m_2} Q_{6m_3}.$$

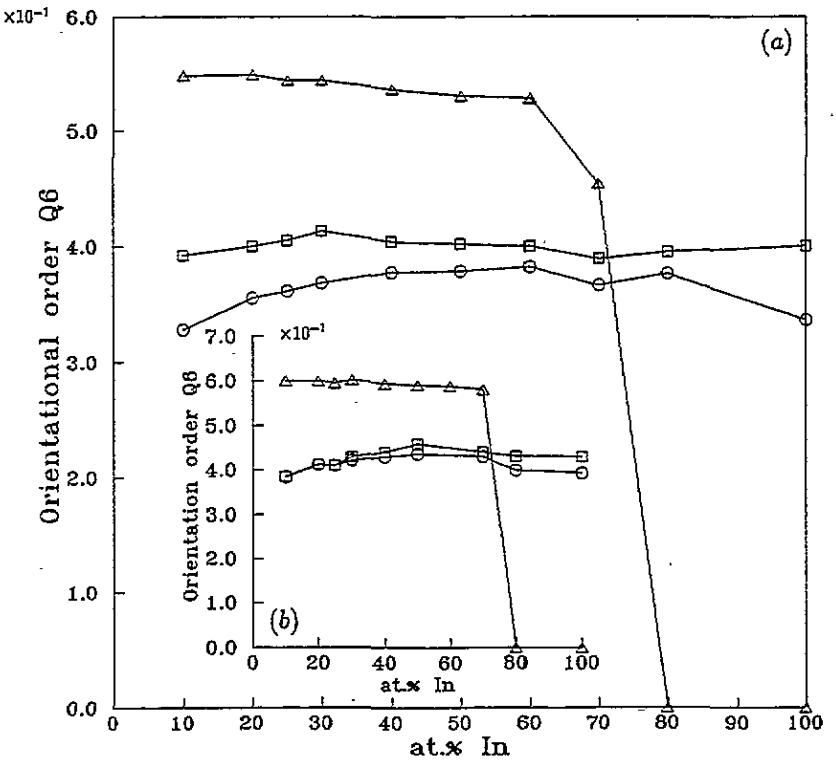

Figure 2. Orientational order parameters Q_6, the quadratic invariant of spherical harmonics, versus In content (*a*) before the mapping and (*b*) after the mapping: △, ICOS Q_6; □, DEF Q_6; ○, TOL Q_6.

This quantity is normalized so that it is independent of the overall magnitude of the $\{Q_{lm}\}$. The order parameters Q_6 and $\hat{W}_6$ measure the icosahedral ordering to some extent, as argued by Steinhardt *et al* [9].

In the present paper, we examine the local symmetry of atomic clusters by a sequence of four integers. Following Honeycutt and Andersen [10], the first integer, either 1 or 2, indicates the cluster type, i.e. whether or not the atoms comprising the root pair are near neighbours. The second integer represents the number of near neighours shared by the root pairs. The third integer represents the number of bonds between the shared neighours. These three numbers are not sufficient to characterize local symmetry uniquely; so a fourth integer, whose value is arbitrary as long as it is used consistently, is added to provide a unique correspondence between numbers and local symmetry as suggested by Honeycutt and Andersen (figure 3 in [10]). From this, if two atoms are within a given cut-off distance, here chosen to equal the position of the first minimum in the appropriate PDF, we say that these two atoms form a bond. Based on the PA formula, the fivefold symmetry bond plus other different kinds of bond can be obtained by computer. The 1551 bonded pairs represent the two root-pair atoms with five common neighbours which have five bonds forming a pentagon of near-neighbour contact. A similar analysis holds for 1441 bonded pairs, 1661 bonded pairs, etc. It is necessary to point out that the number of 1551 bonded pairs in a liquid is a direct measurement of the degrees of icosahedral ordering. By using the PA formula, we can count several polyhedra with various symmetries. If only the centre

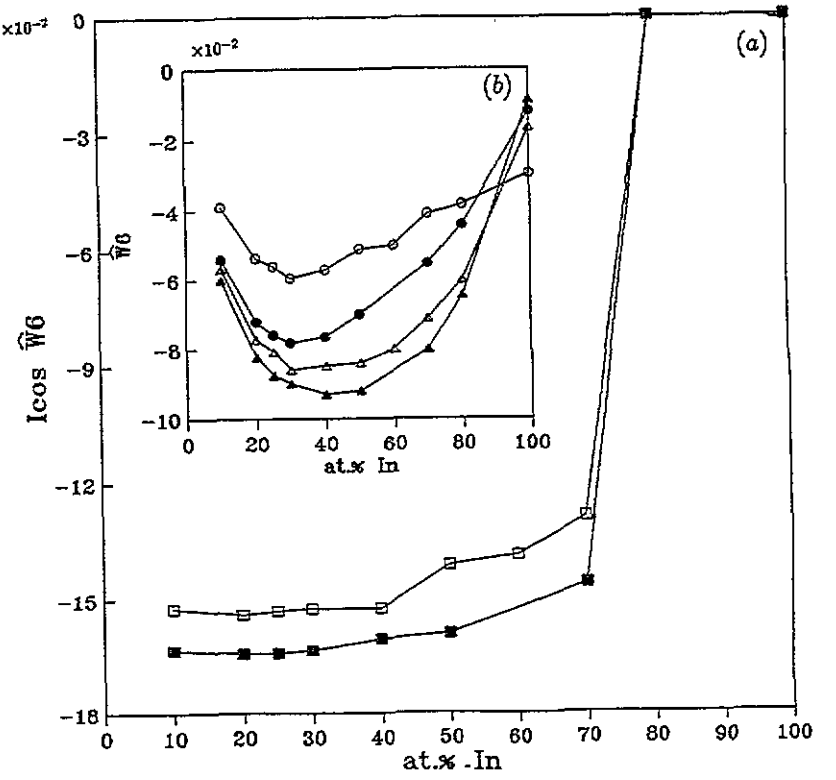

Figure 3. Orientational order parameters $\hat{W}_6$, the third-order invariant of spherical harmonics, versus In content, i.e. (*a*) ICOS $\hat{W}_6$; (■, □) and (*b*) DEF $\hat{W}_6$ (▲, △) and TOL $\hat{W}_6$ (●, ○): ■, ▲, ●, results after the mapping; □, △, ○ results before the mapping.

atom has 12 neighbouring atoms, they are all joined to the centre atom by 12 1551 bonded pairs; we say that they form an icosahedron. Similarly, if the centre atom has 14 (or more) neighbouring atoms, 12 of which are joined to the centre atom by 12 1551 bonded pairs and two (or more) of which are joined to the centre atom by two 1661 bonded pairs, then they define a FK polyhedron with the coordination number $Z = 14$. For other FK polyhedra with different coordination numbers the definition still holds. In the same way, we can define a Bernal hole polyhedron [15]. In addition, a polyhedron consisting of only 1551, 1441 and 1661 bonded pairs is called a defective icosahedron.

5. Results and discussion

5.1. Bond orientational order

Figure 2 represents orientational order parameters, evaluated from equation (4), for binary liquid Li–In alloys both before and after potential mapping. It is clear that the short-range order has been enhanced after mapping onto the minima. In addition it can be seen that the icosahedral order parameters Q_6 (the icosahedral order parameters Q_6 are obtained by calculating Q_6 within the icosahedra defined in section 4 and are hereafter denoted ICOS Q_6) decrease slowly within the In content range from 10 to 70 at.%, i.e.

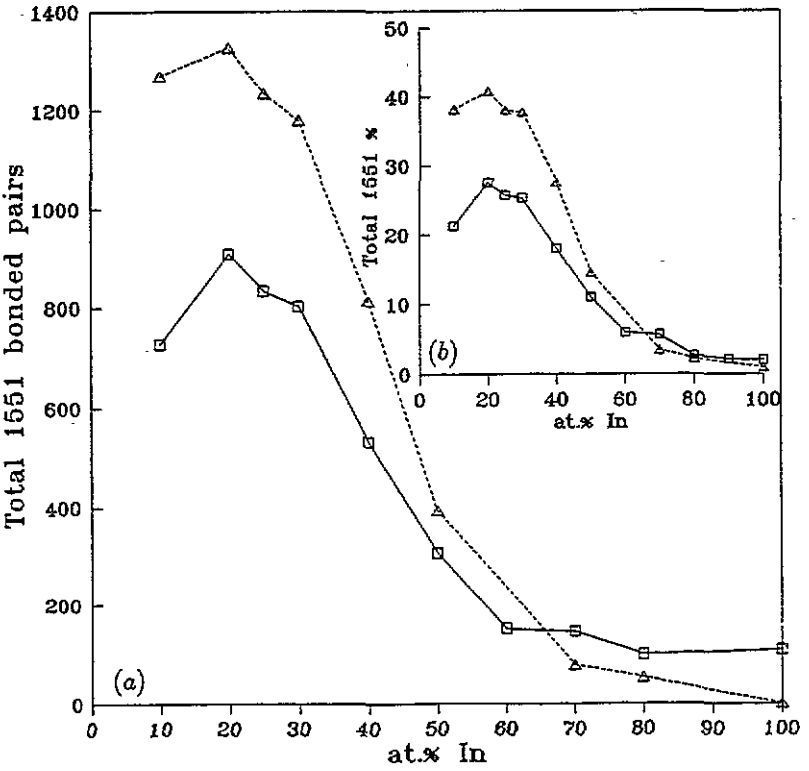

Figure 4. 1551 bonded pairs in binary liquid Li–In alloys, before (□) and after (△) the mapping (*a*) the total numbers in the system; (*b*) the relative number.

no obvious variations in ICOS Q_6 are observed; this primarily suggests that the ICOS Q_6 is not very sensitive to the icosahedral symmetry compared with ICOS $\hat{W}_6$ discussed below (see figure 3). For an In content greater than 70 at.%, ICOS Q_6, however, sharply vanishes, indicating that no icosahedra exists. Other order parameters such as the defective and total icosahedral symmetry Q_6 (in the present paper the defective icosahedral ordering parameters are calculated for defective icosahedral clusters as defined in section 4 and the total icosahedral ordering parameters are calculated for any clusters without distinguishing whether they are icosahedra or not, thus we designate the defective and total icosahedral ordering parameters as DEF Q_6 and TOL Q_6, respectively) vary little throughout the whole composition range of interst. Thus no essential information about structure characteristics can be obtained from these two order parameters; this may be due to the definition of the polyhedra by the PA formula. It also reflets the limitation of the orientational order parameter Q_6. DEF $\hat{W}_6$ and TOL $\hat{W}_6$ are, however, more sensitive to various icosahedral symmetries when compared with Q_6 and the results for $\hat{W}_6$ are shown in figure 3. The more negative $\hat{W}_6$, the more nearly perfect are the icosahedra. For an ideal icosahedron, the absolute value of $\hat{W}_6$ has the maximum 0.169 754 [9]. It is clear from the relatively sharp minimum of TOL $\hat{W}_6$ that icosahedra formed at around 30 at.% In are on average more nearly perfect than those for the other In content ranges before mapping. The corresponding $\hat{W}_6$ for the mapping results are also shown in figure 3(*b*). It is observed that the short-range order of icosahedral symmetries for the whole system can be enhanced by varying TOL $\hat{W}_6$, but the defective icosahedra seem to change slowly as before. Figure 3(*a*) shows ICOS $\hat{W}_6$ versus

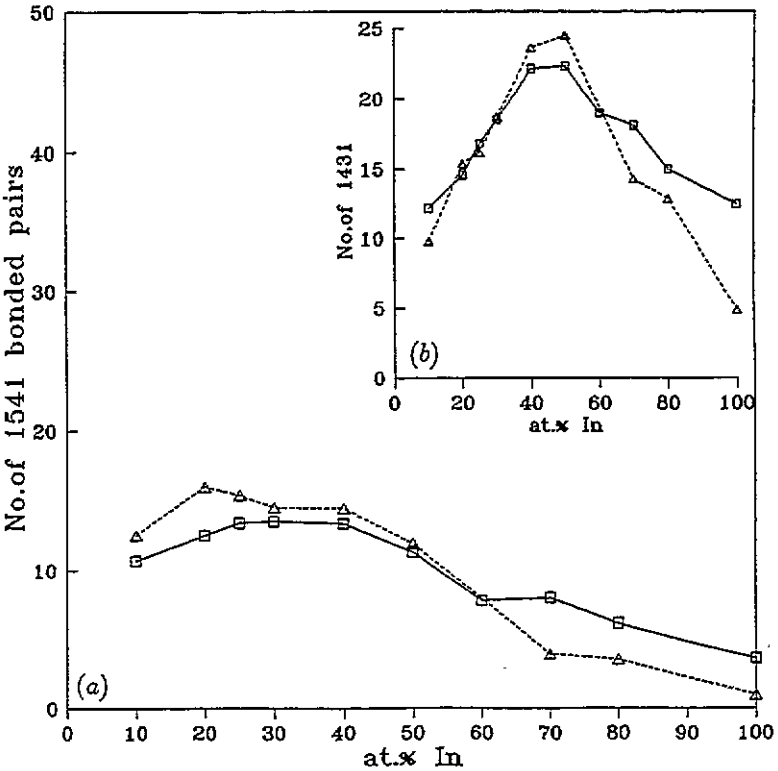

Figure 5. Number 1541 and 1431 bonded pairs versus In content, before (□) and after (△) the mapping.

In content. As expected, the short-range order of icosahedra is enhanced after mapping onto the minima. We say that the third-order invariant of the order parameter ICOS $\hat{W}_6$ is also a direct measurement of the degree of perfection of an icosahedron detected in the simulation. In addition, we find that the most nearly perfect icosahedra in binary Li–In alloys occur at around a lower In concentation of, say, 10 at.% rather than around 30 at.%. This feature should be attributed to the most attractive part of the In–In pair potential, which is the main aim of our research.

5.2. *Pair analysis procedure*

Figures 4(*a*) and 4(*b*) show the total number of 1551 bonded pairs in the whole system and the relative number, respectively. The maximum number of 1551 bonded pairs occurs at around 20 at.% In rather than 10 at.% In. This indicates that, although the most nearly perfect icosahedra are detected at 10 at.% In, it does not mean that 1551 bonded pairs reach the maximum; this may be due to the relatively low In concentrations. This could also explain the number of icosahedra (see figure 6). Thus it confirms that 1551 bonded pairs are a direct measurement of the icosahedral symmetry. In addition, the 1541 and 1431 bonded pairs which describe the characterization of short-range order in a liquid to some extent [14] are also counted and shown in figure 5. One point to note is that the 1541 bonded pairs differ from the 1551 bonded pairs obtained by the PA formula, but this difference cannot be distinguished by the Voronoic cell method. As in the Voronoic cell method, 1551 and

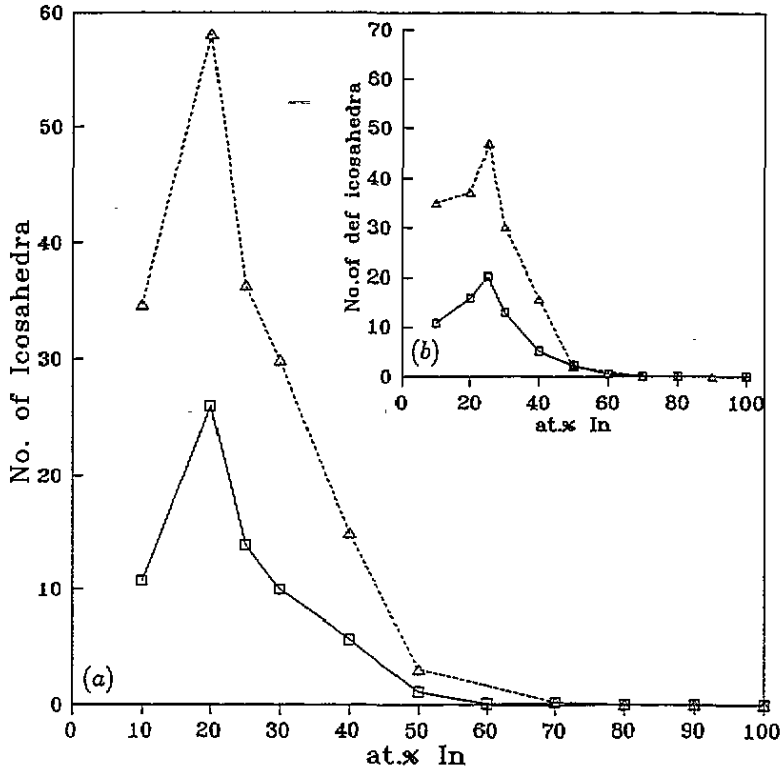

Figure 6. Number of icosahedra and defective icosahedra versus In content, before (□) and after (△) the mapping.

1541 bonded pairs are the same so that the PA formula may be said to be a development of the Voronoic method in some senses. Furthermore, we find that the trends of 1541 and 1431 bonded pairs are similar to those of 1551 bonded pairs, except for the positions at which they have the maximum number of the bonded pairs. Figure 6 gives the relationship between the number of icosahedra and In content. The maximum number of icosahedra is found at around 20 at.% In. This is of course related to the deeper and narrower attractive part of the In–In pair potentials. The results in figure 4 supports the phenomenon. It also tells us that, although the maximum is reached at this In content, the icosahedra detected are not the most nearly perfect. The number of defective icosahedra are also shown in figure 6. We find that the maximum number of defective icosahedra are obtained at around 25 at.% In rather than 20 at.% In, which is different from the results in figures 4 and 5. From the definition on the defective icosahedra by the PA approach, this reflects the competition between the 1551 bonded pairs and other bonded pairs, such as the 1541 and 1431 bonded pairs. Naturally, it demonstrates the fact that the variation in potential distribution induces a change in the symmetries of the bonded pairs. Accordingly, it induces an evolution in the structure of liquids. Double icosahedra (two icosahedra with 19 atoms with one common face) are also counted in our PA program, and figure 7 shows these results. It is found that the number of double icosahedra are greater than the number of icosahedra counted as in figure 6 except for the same trends which two types of polyhedron follow. This prompts us to examine the common faces probably shared by different icosahedra. Figure 7(*b*) gives just this result; it follows the same trends as in figure 6. It demonstrates that the icosahedra

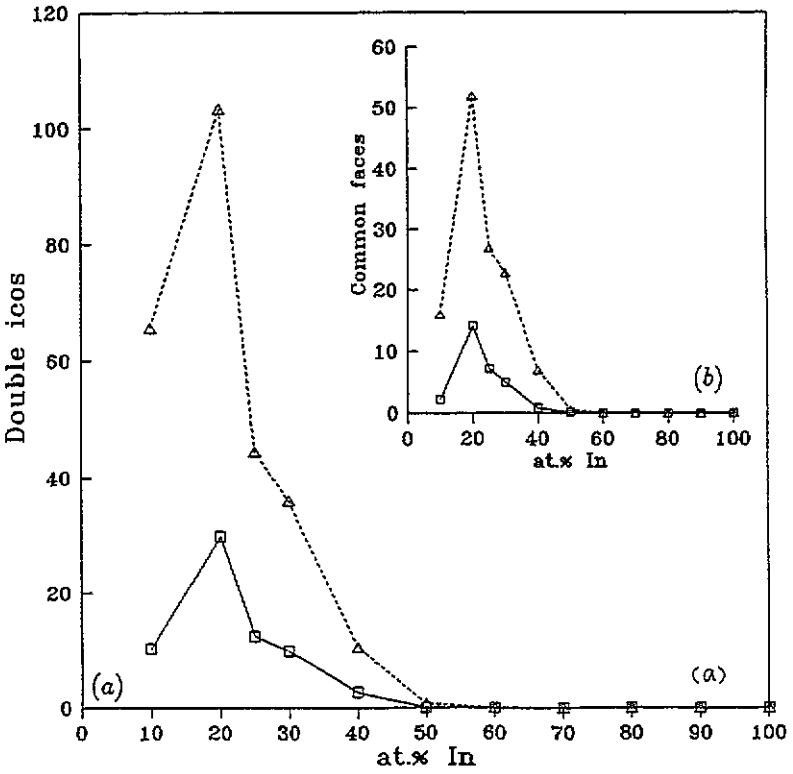

Figure 7. Number of double icosahedra and common faces shared by different icosahedra versus In content, before (□) and after (△) the mapping.

formed in Li–In alloys are mostly double icosahedra with common faces and thus they interpenetrate each other frequently. This may be a characteristic of the structure in Li–In alloys at the present temperature and compositions.

Figure 8 represents the number of FK polyhedra and Bernal polyhedra versus In content. We find that the number of FK polyhedra follows similar trends to figure 6, although the number is much less than the number of icosahedra. Bernal polyhedra, however, have different features, and, within the whole composition range, few Bernal polyhedra occur, even compared with FK polyhedra.

It is well known that the smaller atoms prefer to locate at the centres of icosahedra in order to satisfy the rule for icosahedral packing. In our present case the In atom is larger than the Li atom (but this difference between the two atomic sizes is not very significant). Figure 9 represents the number of both smaller and larger atoms (Li and In) at the centres of icosahedra. It is observed that the number of smaller Li atoms at the icosahedral centres is much less than that of the relative larger In atoms, and the maximum number of atoms at icosahedral centres occurs at around 20 at.% In. If we pay more attention to the distribution of pair potentials in figure 1 and results in figures 4 and 6, then figure 9 is transparently easy to understand. It further indicates that the potential distribution may dominate the arrangement of centre atoms without regard to the requirement of geometrical size. Thus, in our present case, icosahedra formed in Li–In alloys in the vicinity of 20 at.% In are mostly those in which the centre atoms are the relatively larger In atoms.

It is necessary to point out that the number of 1551 bonded pairs before mapping

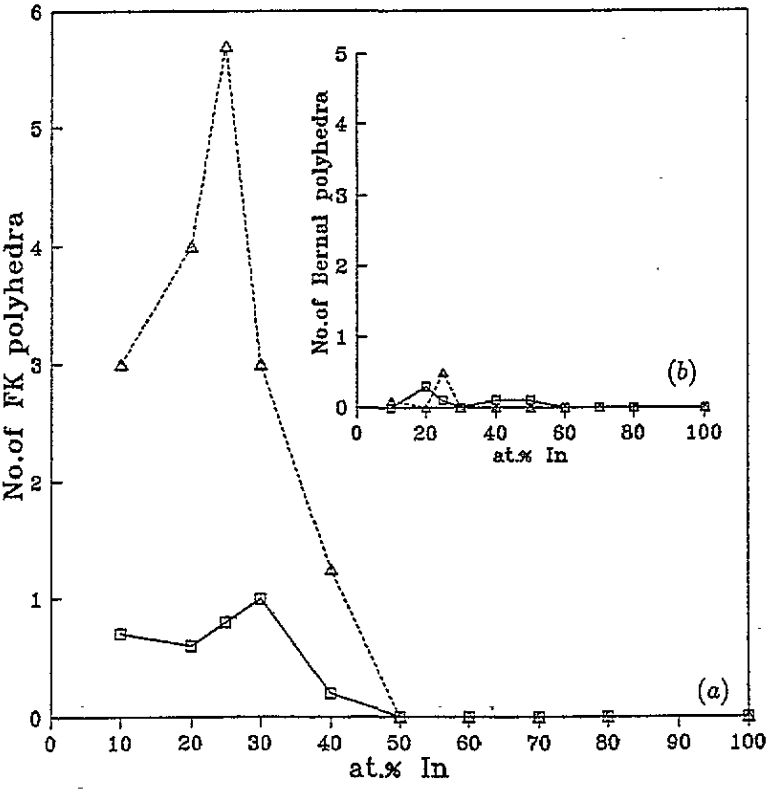

Figure 8. Number of FK polyhedra and Bernal hole polyhedra versus In content, before (□) and after (△) the mapping.

exceeds that after mapping, contrary to the results in the In content range less than 70 at.%. We can explain this with the help of the nature of the inherent structure and the potential distributions of alloys (this phenomenon is also seen in figure 5). Within the In content range from 10 to 70 at.%, especially in the vicinity of 20 at.%, the distribution of pair potentials (the most attractive part of In–In pairs) supports icosahedral symmetry. This conclusion has been confirmed in our previous analysis. It leads to the enhancement of short-range order of icosahedra after mapping. In the In content range from 70 to 100 at.% (pure In metal), however, the In–In pairs become broader and shallower, and the behaviour of pure liquid In occurs; thus the 1311 bonded pairs will play the dominant role [11]. As a result, the number of 1551 bonded pairs sharply decreases more than before mapping. This may be a further test of the concept of the inherent structure. Figure 10 shows both 1321 and 1311 bonded pairs versus In content. Firstly we say that these two bonded pairs differ from each other in the same way as we have explained for 1551 and 1541 bonded pairs. Secondly a feature appears if one pays more attention to figure 10. It is observed that within the whole composition range the number of 1321 bonded pairs before mapping is more than that after mapping; this gives rise to the conclusion that the pair potentials of Li–In alloys do not support 1321 bonded pairs in some senses from the viewpoint of the inherent structure. In figure 10, we find another feature which may differ from 1321 bonded pairs. If we consider the In content range from 10 to 50 at.%, as explained in the previous section, pair potentials do not support 1311 bonded pairs within the In content range from

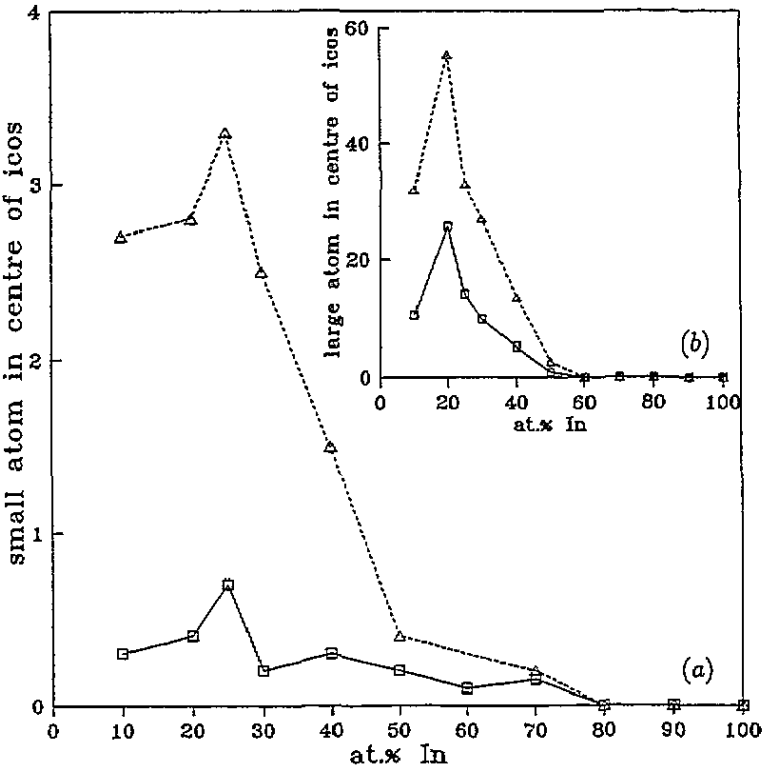

Figure 9. Number of smaller (Li) and larger (In) atoms at the centres of icosahedra versus In content, before (□) and after (△) the mapping.

60 to 70 at.%; the competition may get the balance. This reflects the fact that these two values achieve equilibrium. When the In content exceeds 70 at.%, 1311 bonded pairs play the dominant role in the system. This may be another characteristic of the structure of liquid Li–In alloys.

6. Conclusions

Based on the effective interatomic potentials derived from the GNMPs, MD simulations combined with potential mapping techniques have been performed to investigate the characterization of structures in binary liquid Li–In alloys. Our results demonstrate that the orientational order parameter $\hat{W}_6$, which is a third-order invariant of the spherical harmonics, is more sensitive to the icosahedral symmetry than is the quadratic invariant Q_6 and, after mapping the potential minima, the short-range order of the structure has been enhanced. Within the In content range greater than 70 at.% In, no icosahedra exists, and the maximum number of icosahedra formed in binary Li–In alloys is found at around 20 at.% In and the characteristics of 1551 bonded pairs confirm this conclusion; the reason may be attributed to the potential distribution, e.g., relatively deeper and narrower attractive part of $V_{\mathrm{In-In}}$. In addition, FK polyhedra and Bernal polyhedra are also counted, and the FK polyhedra follow similar trends to the icosahedra. Bernal polyhedra, however, behave differently when compared with the behaviour of icosahedra.

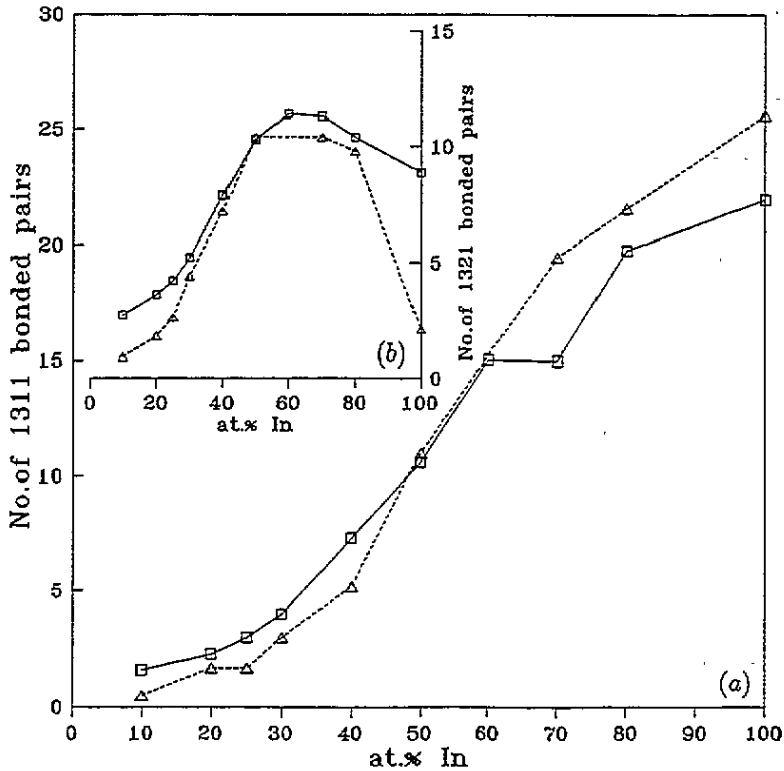

Figure 10. Number of 1311 and 1321 bonded pairs versus In content, before (□) and after (△) the mapping.

In our present study, the results further show that 1311 bonded pairs dominate when the In content is greater than 70 at.%; this may be due to the behaviour of pure In metal. For an In content greater than 70 at.% In, the number of 1551 bonded pairs before mapping exceeds the result after mapping, leading to the conclusion that the potential at this composition naturally supports 1311 bonded pairs rather than 1551 bonded pairs; similar phenomena for 1541 and 1431 bonded pairs are also observed. The maximum number of double icosahedra is greater than that of single icosahedra; this can be confirmed from the relative larger number of common faces shared by different icosahedra. The number of larger In atoms located at the centres of icosahedra is much greater than that of smaller Li atoms. The reason may be due to the more attractive part of the potential for In–In pairs.

Acknowledgments

We would like to thank Professor S Wang, at Waterloo University of Canada, for helpful discussions and for providing MD computer codes in our research. Financial support provided by the Natural Science Foundation of China is gratefully acknowledged.

References

[1] Hafner J, Kahl G and Pasturel A 1987 *NATO ASI Series E* (Dordrech, Boston: Nijhoff) p 164

[2] Hafner J and Pasturel A 1985 *J. Physique* **46** C8 367
[3] Stillinger F H and Weber T A 1984 *Science* **356**
[4] Stillinger F H and Weber T A 1984 *J. Chem. Phys.* **80** 4434
[5] Stillinger F H and Weber T A 1989 *J. Chem. Phys.* **81** 5089
[6] Stillinger F H and Weber T A 1985 *Phys. Rev.* B **31** 5202
[7] Broughton J Q, Gilmar G H and Weeks J D 1982 *Phys. Rev.* B **35** 4651
[8] Steinhardt P J, Nelson D R and Ronchetti M 1981 *Phys. Rev. Lett.* **47** 1275
[9] Steinhardt P J, Nelson D R and Ronchetti M 1981 *Phys. Rev.* B **28** 784
[10] Honeycutt J D and Andersen H C 1987 *J. Phys. Chem.* **91** 4950
[11] Lu J and Szpunar J A 1992 *J. Chem. Phys.* **97** 1313
[12] Liu C F, Wang S and Lu J 1992 *J. Chem. Phys.* **97** 2694
[13] Qi D W, Lu J and Wang S 1992 *J. Chem. Phys.* **96** 513
[14] Liu C F and Wang S 1992 *J. Phys. C: Solid State Phys.* 4 6729
[15] Qi D W and Wang S 1991 *Phys. Rev.* B **44** 884
[16] Liu R S, Qi S W and Wang S 1992 *Phys. Rev.* B **45** 451
[17] Liu R S and Wang S 1992 *Phys. Rev.* B **46** 12001
[18] Li D H, Moore R A and Wang S 1986 *Can. J. Phys.* **64** 75
[19] Li D H, Moore R A and Wang S 1986 *Can. J. Phys.* **64** 852
[20] Wang S and Lai S K 1980 *J. Phys. F: Met. Phys.* 7 1439
[21] Alder B J and Wainwright T E 1957 *J. Chem. Phys.* **27** 1207
[22] Verlet L 1967 *Phys. Rev.* **159** 98
[23] Frank F C 1952 *Proc. R. Soc.* A **215** 43
[24] Nelson D R and Toner J 1981 *Phys. Rev.* B **24** 363